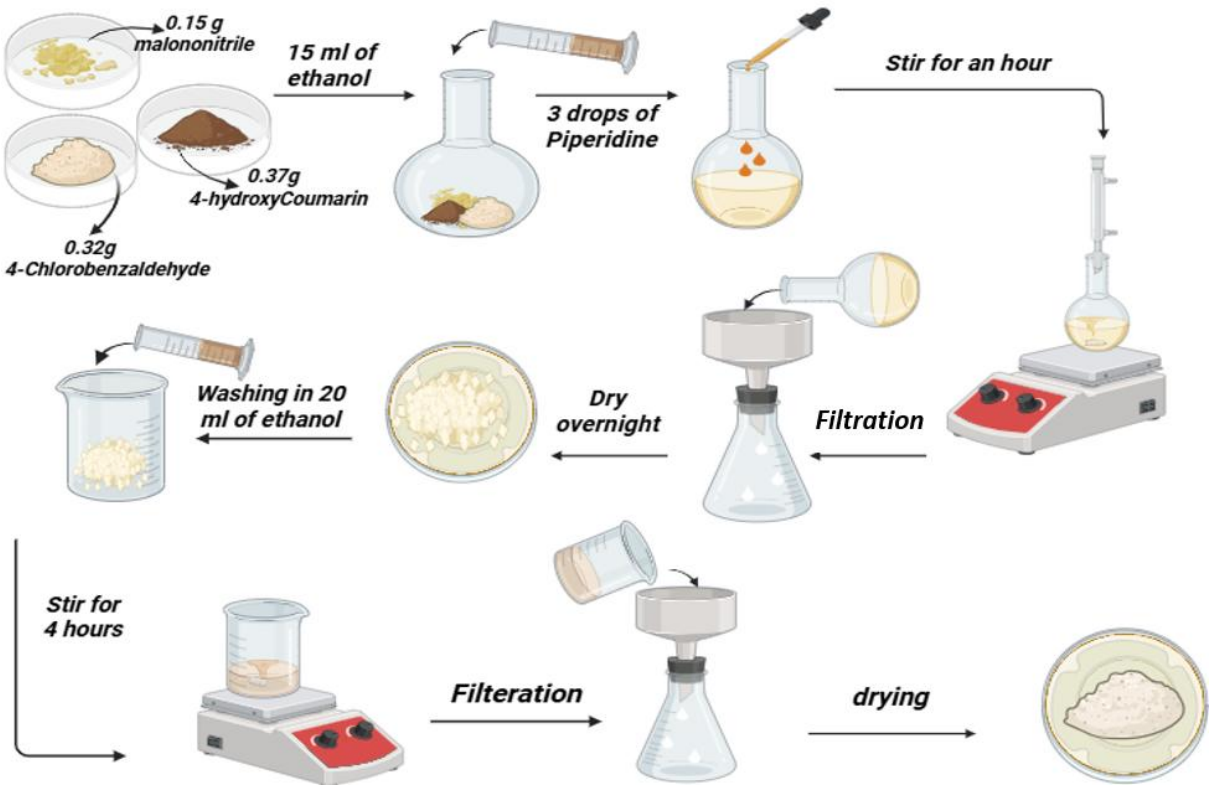
Figure S1: Schematic illustration of the synthesis procedure of 2-amino-4-(4-chlorophenyl)-5-oxo-4H,5H-pyrano[3,2-c]chromene-3-carbonitrile (ACLPh-PC-3-CN). The ligand was synthesized via a one-pot multicomponent reaction of 4-chlorobenzaldehyde, malononitrile, and 4-hydroxycoumarin in ethanol, catalyzed by piperidine, followed by filtration, ethanol washing, and drying.



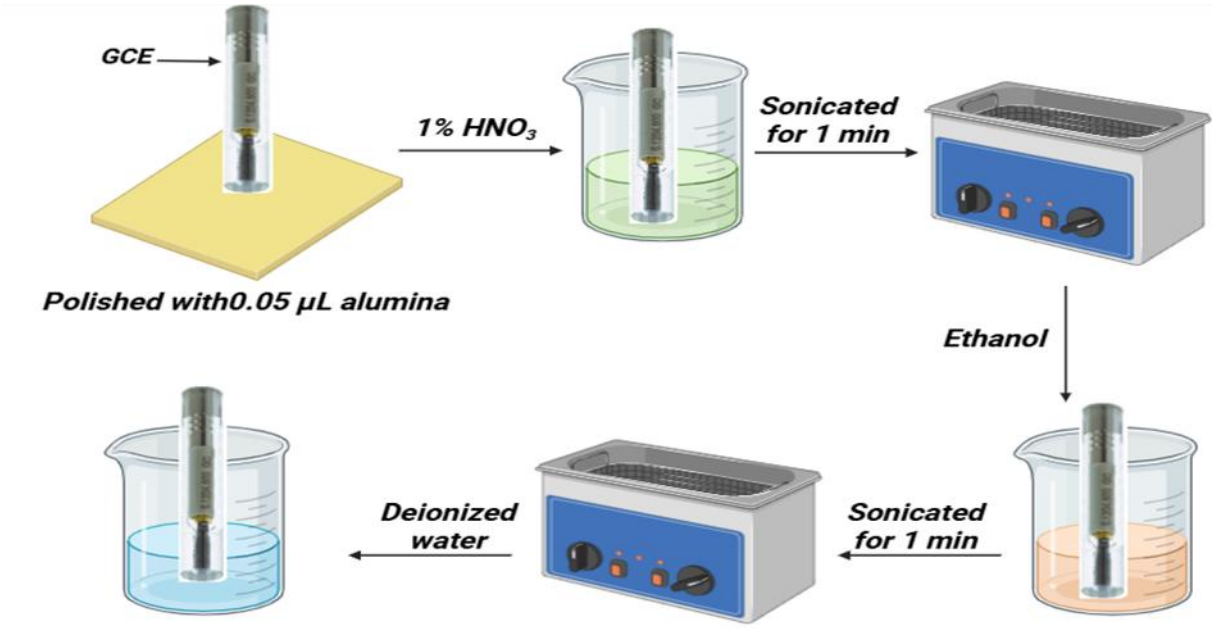


Figure S2: Cleaning and pretreatment procedure of the glassy carbon electrode prior to modification.

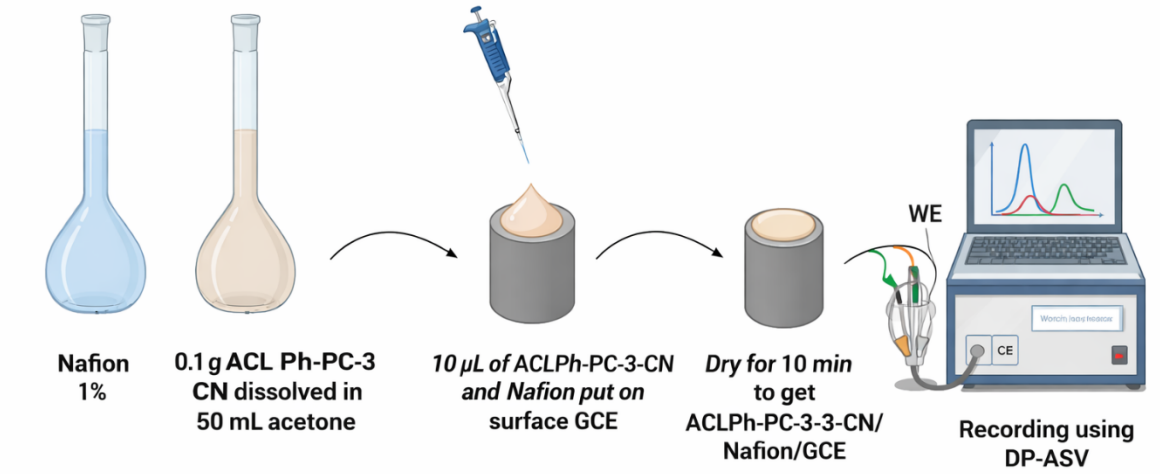


Figure S3: Schematic representation of the fabrication procedure of the ACLPh-PC-3-CN/Nafion modified glassy carbon electrode (ACLPh-PC-3-CN/Nafion/GCE). A solution of ACLPh-PC-3-CN in acetone was drop-cast onto the pretreated GCE surface together with Nafion solution, followed by air drying to form a uniform film prior to electrochemical measurements using DP-ASV.

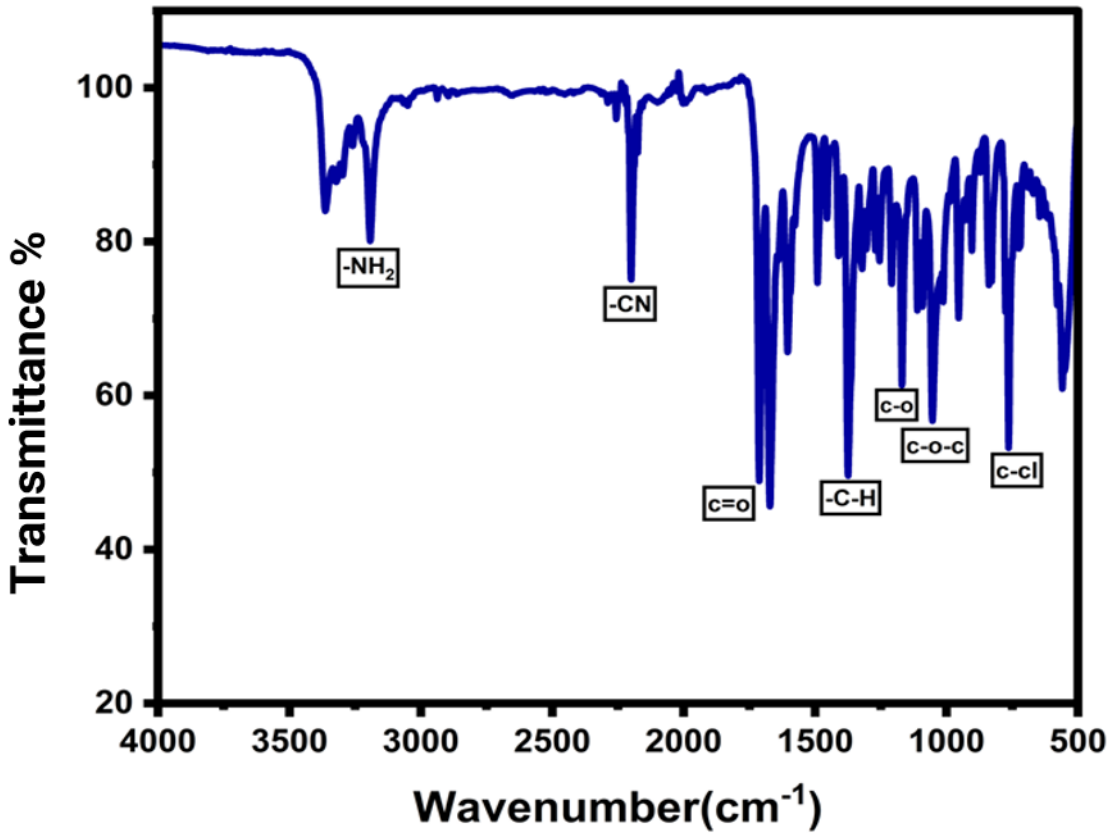
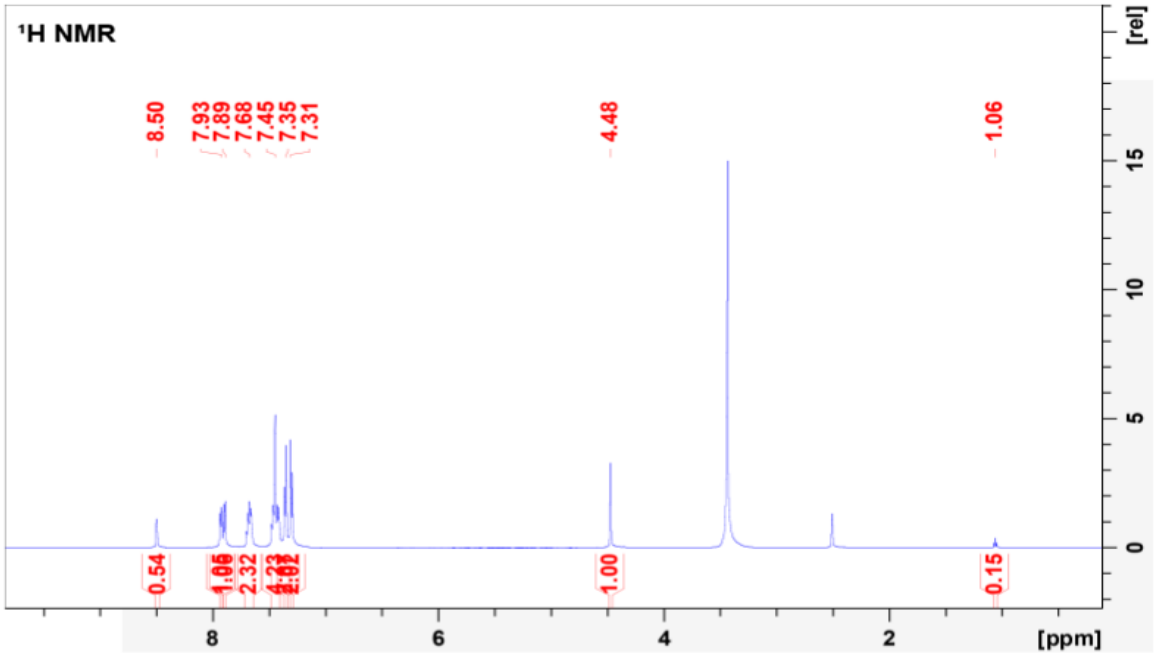


Figure S4. FT-IR spectrum of ACLPh-PC-3-CN (500–4000 cm^{-1}).



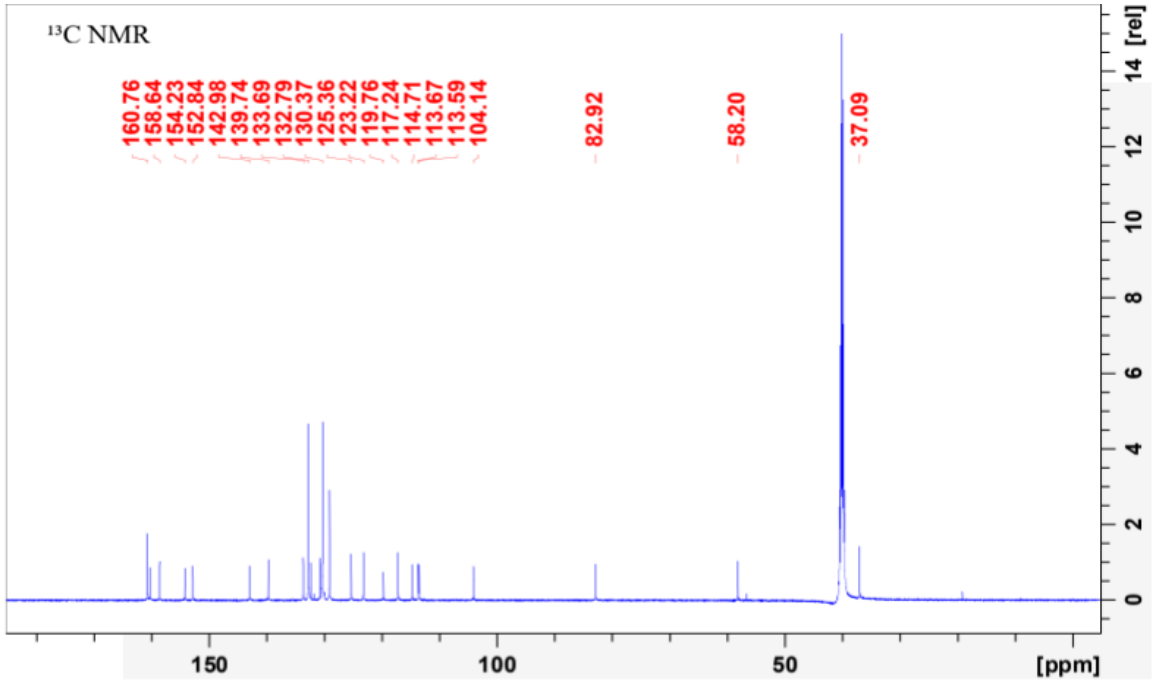


Figure S5. (A) ^{1}H NMR and (B) ^{13}C NMR spectra of ACLPh-PC-3-CN in DMSO-d_6.

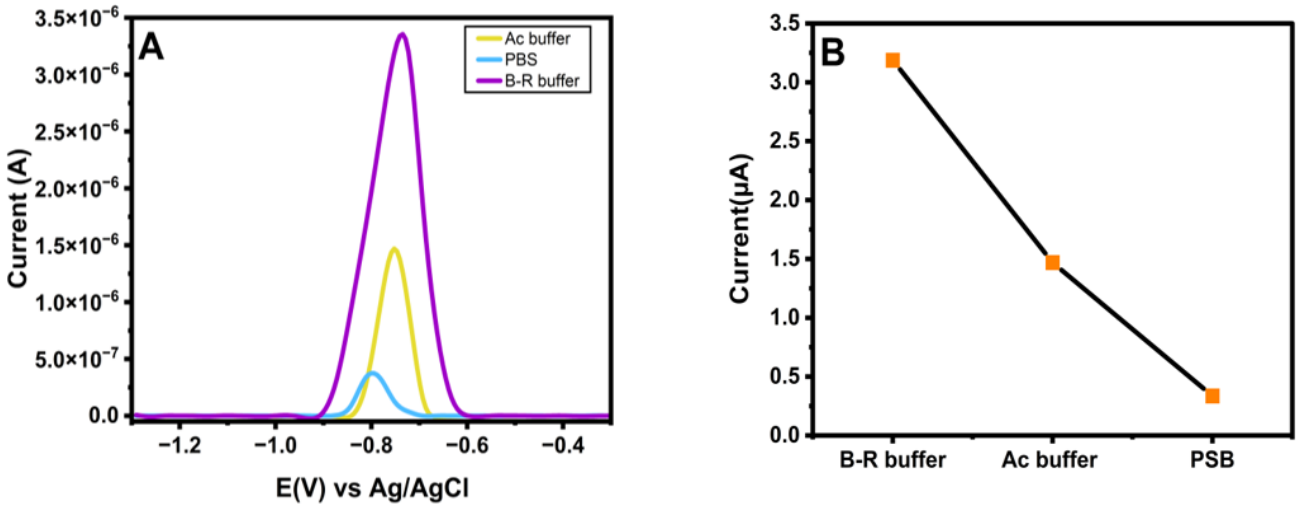


Figure S6 (A and B): DP-ASV voltammogram at different supporting electrolytes (A) and influence of the supporting electrolytes on the peak current of Cd(II) ions (4.8×10^{-6} mol L^{-1}) at ACLPh-PC-3-CN/Nafion/GCE vs the Ag/AgCl electrode (B). Experimental conditions: deposition potential – 0.6 V, deposition time 120 s, pulse amplitude 50 mV.

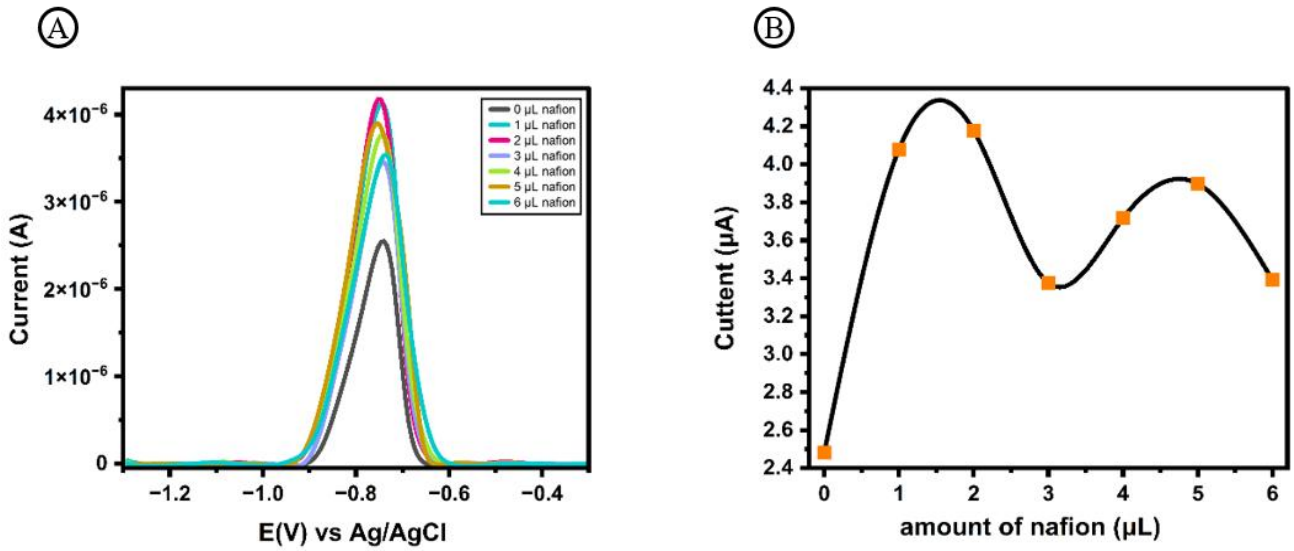


Figure S7 (A and B): Effect of Nafion amount on the DP-ASV response of Cd(II) (4.8×10^{-6} mol L^{-1}) at the ACLPh-PC-3-CN/Nafion modified electrode: (A) DP-ASV voltammograms recorded with different Nafion volumes (0–6 µL); (B) corresponding variation of anodic peak current with Nafion volume. Experimental conditions: deposition potential −0.6 V, deposition time 120 s, B-R buffer solution at pH 4.

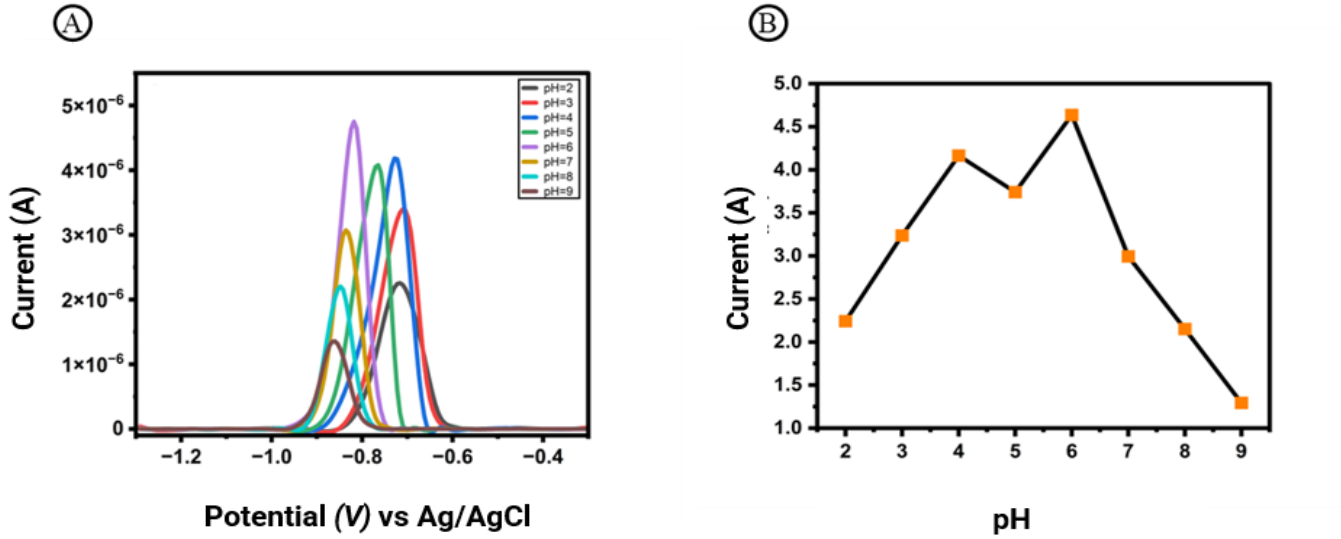


Figure S8 (A and B): Effect of pH on the DP-ASV response of Cd(II) (4.8×10^{-6} mol L^{-1}) at the ACLPh-PC-3-CN/Nafion modified electrode: (A) DP-ASV voltammograms recorded at different pH values (2–9); (B) corresponding variation of anodic peak current with pH. Experimental conditions: deposition potential −0.6 V, deposition time 120 s, pulse amplitude 50 mV, B-R buffer solution.

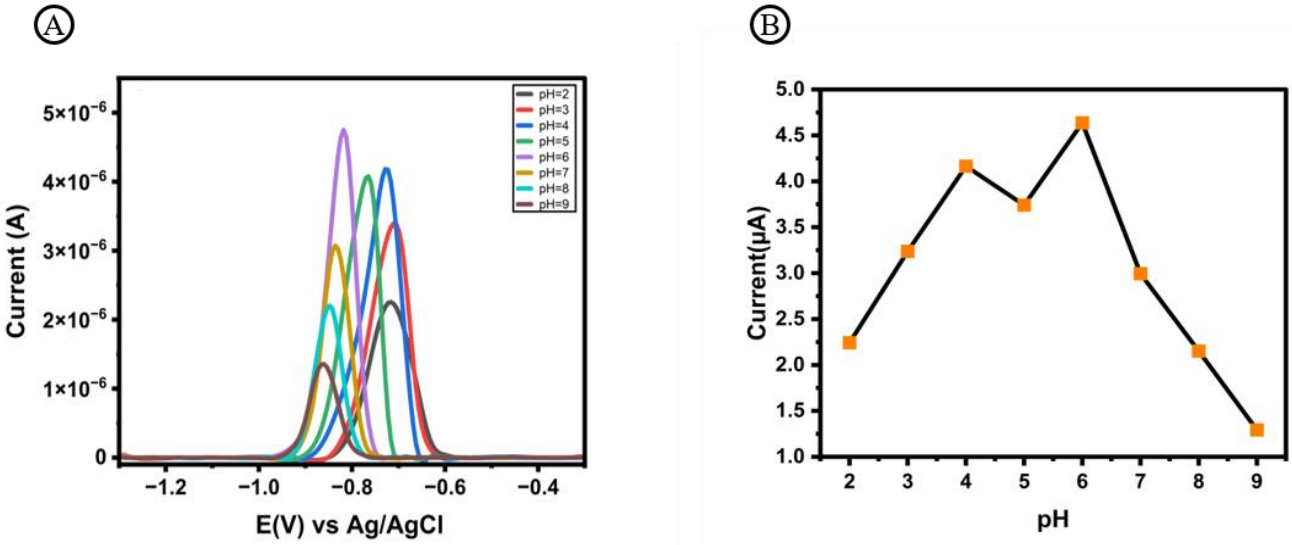


Figure S9 (A and B): Effect of deposition potential on the DP-ASV response of Cd(II) (4.8×10^{-6} mol L^{-1}) at the ACLPh-PC-3-CN/Nafion modified electrode: (A) DP-ASV voltammograms recorded at different deposition potentials; (B) corresponding variation of anodic peak current with deposition potential. Experimental conditions: deposition time 120 s, pulse amplitude 50 mV, B-R buffer solution at pH 6.

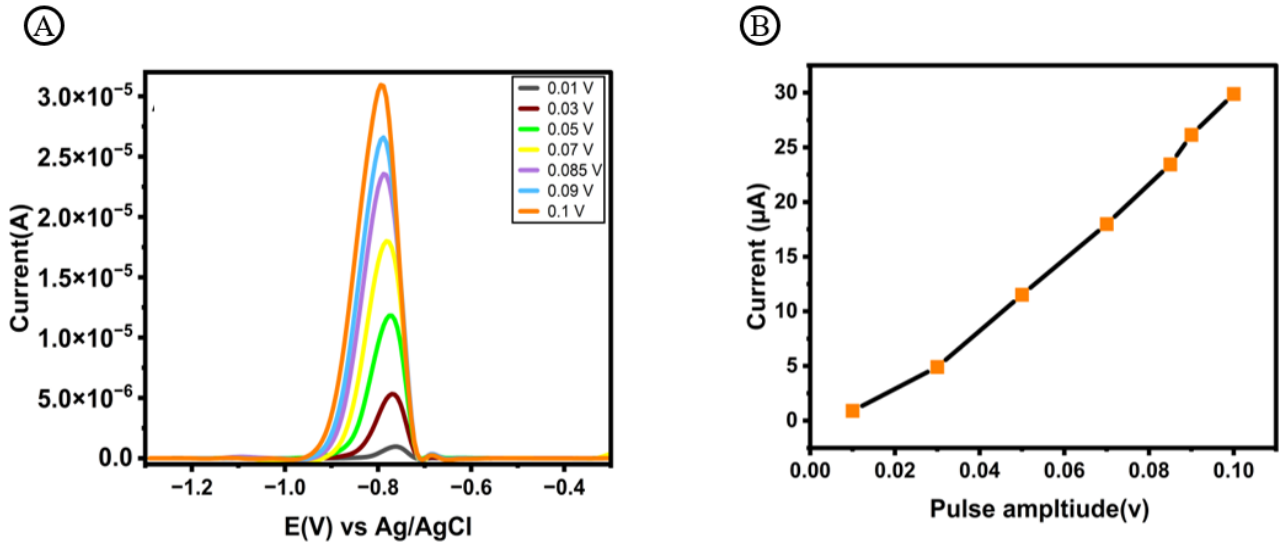


Figure S10 (A and B): Effect of pulse amplitude on the DP-ASV response of Cd(II) (4.8×10^{-6} mol L^{-1}) at the ACLPh-PC-3-CN/Nafion modified electrode: (A) DP-ASV voltammograms recorded at different pulse amplitudes (10–100 mV); (B) corresponding variation of anodic peak current with pulse amplitude. Experimental conditions: deposition potential −1.35 V, deposition time 120 s, B-R buffer solution at pH 6.

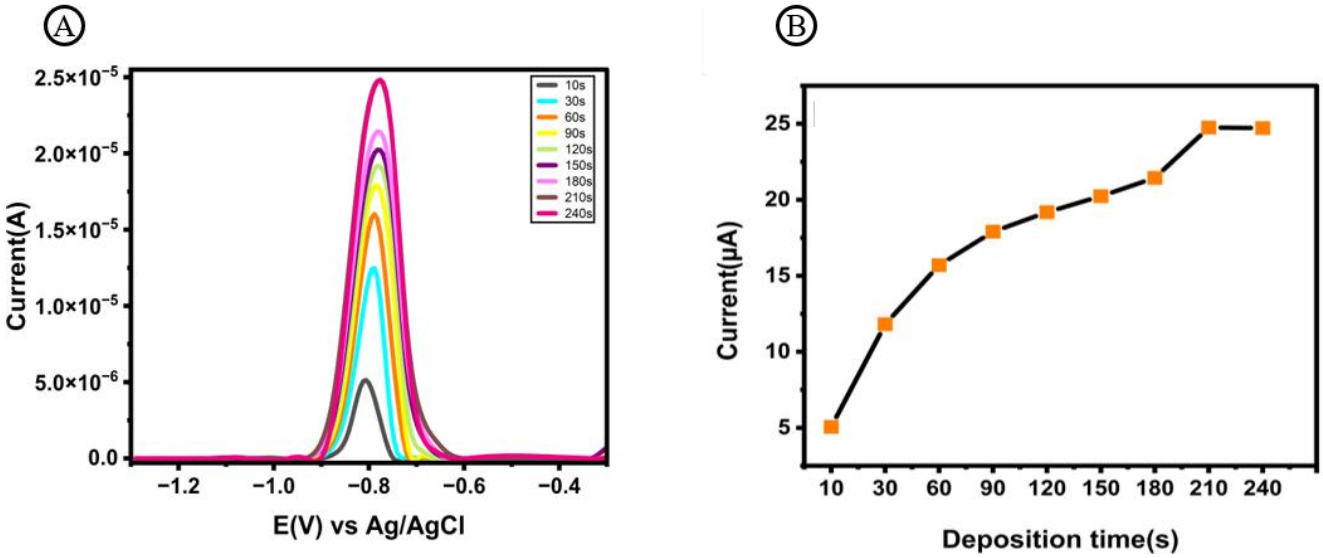


Figure S11 (A and B): Effect of deposition time on the DP-ASV response of Cd(II) (4.8×10^{-6} mol L^{-1}) at the ACLPh-PC-3-CN/Nafion modified electrode: (A) DP-ASV voltammograms recorded at different deposition times; (B) corresponding variation of anodic peak current with deposition time. Experimental conditions: deposition potential −1.35 V, pulse amplitude 70 mV, B-R buffer solution at pH 6.

Table S1: Influence of potential interfering ions on the determination of Cd(II) (4.8×10^{-6} mol L^{-1}) using the ACLPh-PC-3-CN/Nafion modified electrode

Interfering species	Concentration ratio (Interferent:Cd(II))	Change in Cd(II) peak current (%)
Pb^{2+}	10 : 1	< 5
Cu^{2+}	10 : 1	< 5
Zn^{2+}	10 : 1	< 4
Ni^{2+}	10 : 1	< 4
Hg^{2+}	10 : 1	< 5
Na^{+}	50 : 1	negligible
K^{+}	50 : 1	negligible
Ca^{2+}	50 : 1	negligible
Mg^{2+}	50 : 1	negligible
Cl^{-}	100 : 1	negligible
NO_3^{-}	100 : 1	negligible
SO_4^{2-}	100 : 1	negligible
Triton X-100	100 : 1	negligible
Ag^{+}	100 : 1	< 5
Co^{2+}	100 : 1	< 5
Mn^{2+}	100 : 1	< 5